1-1-2004

AC Frequency Dependence of Electroluminescent ZnS Phosphor Panel Color

Farrah Shantell Boggess-Machado

AC FREQUENCY DEPENDENCE OF ELECTROLUMINESCENT ZnS PHOSPHOR PANEL COLOR

Thesis submitted to
The Graduate College of
Marshall University

In Partial Fulfillment of the
Requirements for the Degree of
Master of Science

by

Farrah Shantell Boggess-Machado

Dr. Michael Norton, Committee Chairperson
Dr. William Price
Dr. Robert Morgan

Marshall University

June 2004

ABSTRACT

In this study, electroluminescent panels manufactured by Meadow River Enterprises were used to study the AC frequency dependence of their color. A project was developed to acquire their emittance color at various frequencies. Three frequencies were selected for the investigation. Data, obtained by measuring the spectrum at a constant excitation frequency, were taken for each of the three standard frequencies: 200 Hz, 1500 Hz, and 20 kHz. In general the higher the frequency, the bluer the emittance color of the panel. The lower the frequency, the more green the panel became. An explanation for this phenomenon, the frequency dependence of the emission color, is suggested using a model for the electronic structure of Cu doped ZnS. It can be concluded that the blue emission is a two step process, while the green emission is a one step process according to the model used in this project.

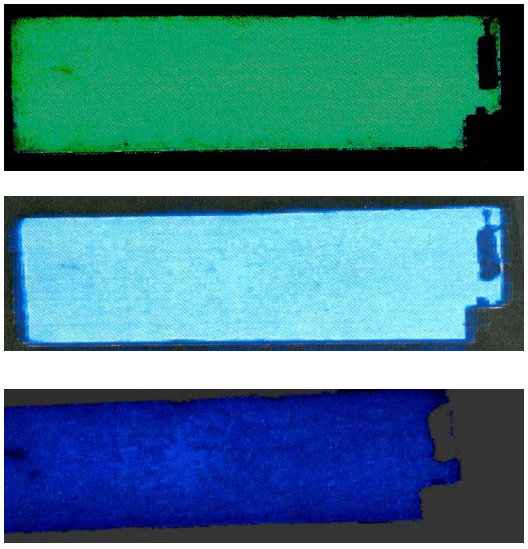

200 Hz

1500 Hz

20 kHz

ACKNOWLEDGMENTS

The author wishes to thank Meadow River Enterprises for supplying the samples for this study. Support from the United States Department of Transportation funded Appalachian Transportation Institute at Marshall University is also acknowledged. The author also expresses special thanks to Dr. Norton, Dr. Price, and Dr. Morgan for the considerable amount of help, patience, and knowledge afforded to this project. Also, thanks to Ava Dykes for her constant reassurance, the West Virginia State Police for allowing work time for the completion of this project, and the faculty of the Marshall University Department of Chemistry. Last but not least, the author wishes to thank her parents Ray and Vicki Boggess, her husband Keith, and her beautiful daughter Delaney.

TABLE OF CONTENTS

LIST OF FIGURES

LIST OF TABLES

CHAPTER I

Introduction

The behavior of phosphors, such as zinc sulfide, has been studied in a strong electric field since 1920. At that time, Gudden and Pohl discovered that a light flash was emitted by a ZnS-Cu phosphor if an electric field was applied during the afterglow while studying the photoconductivity of ZnS (1). In 1936 Georges Destriau discovered the “electroluminescence” effect or “Destriau-effect”; some copper activated zinc sulfide phosphors luminesced in strong AC fields (2).

Figure 1 illustrates the construction of an electroluminescent cell. This type of cell is considered a plane condenser with dielectric losses; part of the dissipated energy is converted into light (1).

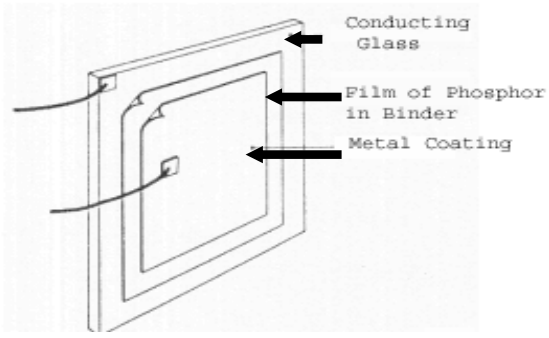

Figure 1. Diagram of an electroluminescent cell.

The early phosphors that Destriau made did not have any halides present. It is now known that high copper content improves the electroluminescence. Thorington observed very early on that many sulfide phosphor powders became electroluminescent when placed between electrodes and the container

evacuated. He then concluded that the state of the surface is important for electroluminescence excitation (3). Zalm showed that it is possible to render a photoluminescent but non-electroluminescent ZnS: Cu phosphor electroluminescent by simply depositing a small amount of copper on the surface (1). Lehmann observed that many non-electroluminescent phosphors (including many non- sulfide types) become electroluminescent when mixed with a metallic or semi-conducting powder; he called this “contact electroluminescence” (3).

ZINC SULFIDE STRUCTURES

Zinc sulfide and related compounds form the basis for many photoluminescent and cathodoluminescent phosphors. They are also the most efficient electroluminescent phosphors known. Zinc sulfide exists in two forms: a low-temperature cubic (sphalerite or zincblende) structure and a high-temperature hexagonal (wurtzite) structure. The sphalerite structure can be derived from a cubic close packing of ions, while the wurtzite structure is derived from a hexagonal close packing scheme. Figure 2 shows each crystal structure. This situation is not that simple however, because the difference in energy of the two structures is small. It has been reported that electroluminescent material must contain both sphalerite and wurtzite phases(4). The wurtzite type structure predominates when the bonding is primarily ionic whereas the more covalent systems favor the sphalerite form. The nature of the end product is usually dependent on heat treatment temperature, cooling profile, and cooling atmosphere since the heat treatment of zinc sulfide samples containing copper

as a dopant leads to significant changes (4). Table 1 provides the energy band gap for several of the Group II-VI compounds (3). Appendix A shows the calculations of the bandgap wavelengths for hexagonal and cubic structures.

It is extremely useful to compare the properties of the different phases from a device applications point of view. For example, one phase can be more suitable than another in certain applications. The cubic phase of ZnS is not grown as easily as the hexagonal phase, thus making the hexagonal phase more appealing for EL device applications (5).

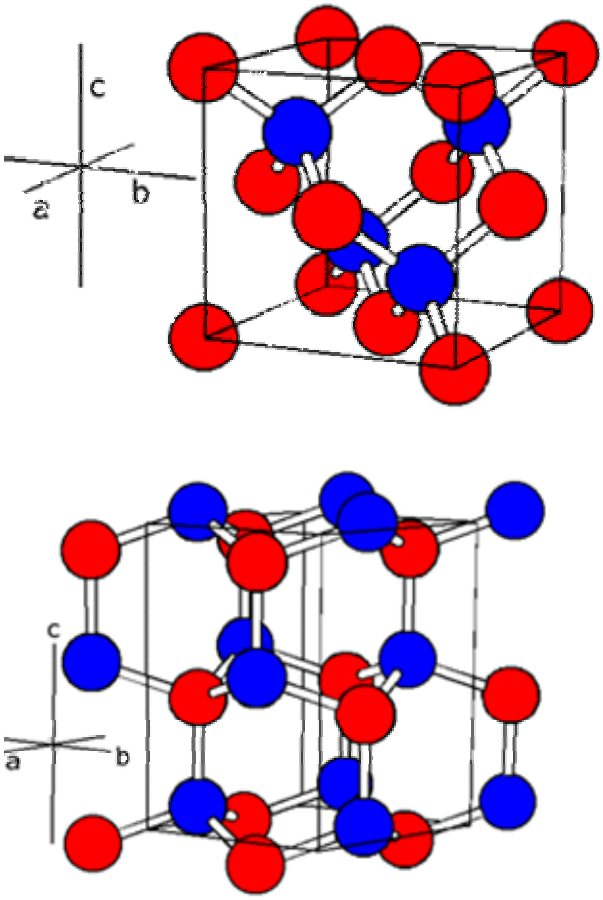

Figure 2. The sphalerite or zincblende crystal structure of ZnS (top)(6). The wurtzite crystal structure of ZnS (bottom)(7).

Compound	Lattice Structure	Band Gap (eV)	Band Gap (Å)
ZnS	Hexagonal	3.70	3350
ZnS	Cubic	3.64	3410
ZnO	Hexagonal	3.20	3880
ZnSe	Cubic	2.60	4770
CdS	Hexagonal	2.43	5100
ZnTe	Cubic	2.15	5780
CdSe	Hexagonal	1.74	7115
CdTe	Cubic	1.42	8710

Table 1. Structure properties of the Group II-VI Compounds.

Zinc sulfide in common with most (but not all) inorganic phosphors, must be "activated" by suitable impurities in order to produce luminescence. Zinc sulfide may be activated for photoluminescent emission by a variety of elements including: Cu, Ag, Au, P, As, Sb, Pb, Mn, V, Fe, Na, Li, Ga, In, Tl, Sc, and rare earths. Zinc vacancies in the lattice should be added to these since they are assumed to be responsible for the "self-activated emission."

The concentration of many of these activator elements in the ZnS lattice is usually limited due to their limited solubility unless another element called the coactivator is introduced at the same time. The coactivator is usually a halide (Cl, Br, I) or a trivalent ion (Al, Ga, In, etc.). The coactivator, however, does not only affect the solubility of the activator. An electron is transferred to or from the coactivator to effect the charge compensation when it is incorporated into the

lattice. The coactivator centers can capture electrons and subsequently release them under thermal action or some other form of stimulation when the phosphor is excited and electrons appear in the conduction band. In the same manner that the activators serve as hole traps or acceptors and influence many phosphor properties in addition to electroluminescence, the coactivator centers act as electron traps or donors.

The situation is far from simple with an activator such as Cu in ZnS. The photoluminescent emission of ZnS: Cu is usually either blue (peak at about 4550Å) or green (peak at 5200Å) or a combination of the two depending upon other conditions. The green emission is favored at higher coactivator/activator ratios (3). Figure 3 indicates the correspondence between the color of visible light and the wavelengths as measured in nanometers.

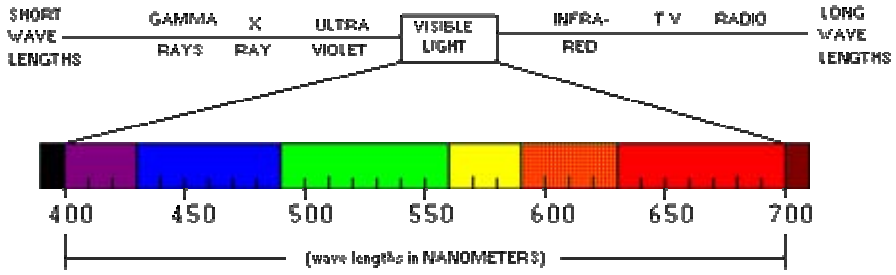

Figure 3. The visible light spectrum showing the difference between the blue wavelength and the green wavelength (8).

PREPARATION OF ZnS

One procedure, which may be used to produce small laboratory samples, is described below (the formulation results in a green-emitting phosphor): (1,3)

1) Slurry 10 grams luminescent-grade ZnS (free of halide) with 3 mL of 0.2N $Cu(CH_3COO)_2$ solution (corresponding to 0.6 atom % Cu) and 1.7 mL of 0.2N NH_4Cl solution (corresponding to 0.34 atom % Cl). Dry at 120ºC and mix with 0.5 grams purified sulfur.

2) Place mix in transparent silica tube (volume about 13 mL) sealed at one end and with close-fitting cap consisting of nitrogen. After flushing, fire at 950ºC for 90 minutes with a continuous flow of nitrogen.

3) Crush with 0.5 grams purified sulfur and repeat step (2).

4) Crush, wash with 10% NaCN (+ NaOH) solution, wash with H_2O until neutral, wash with alcohol, dry and sieve.

One important step for decreasing the conductivity and improving the performance of electroluminescent lamps or cells is the procedure of washing the phosphors in sodium (or potassium) cyanide to remove the excess Cu_2S from the surface, which is now a standard technique. Thiourea, sodium thiosulfate, or sodium thiocyanate are less toxic and may be used but are generally less effective (3).

Another method of preparation is washing a luminescent ZnS type phosphor with a solution of copper salt. Copper is deposited on the zinc sulfide from the solution as copper sulfide. The product then shows electroluminescence after drying thoroughly (1).

Introducing copper into the zinc sulfide phosphors produces green and blue fluorescence. By varying the atmosphere and temperature of firing, different

concentrations of these centers are produced (9). At temperatures greater than 1000°C, the formation for green centers is favored by high HCl concentration. Low HCl content favors the relative concentration of blue copper centers (10). Khomchenko found that, in general, the relative intensity and maximum location of the bands are determined by the growth conditions (11).

FLUORESCENT CENTERS AND TRAPS

The activators in zinc sulfide can be separated into two distinct types:

(a) activators of the “fundamental” type

(b) activators of the “characteristic” type

Univalent elements, such as Cu and Ag, are considered to be the “fundamental” type activator since they give rise to the presence of energy levels (in the unexcited state occupied by an electron) between the valence and the conduction band. Monovalent activator ions, such as Cu^{+}, Ag^{+}, Au^{+}, and Li^{+}, will normally occupy lattice sites and can be incorporated into zinc sulfide only by charge compensation.

While positive monovalent ions act as negative disturbances in ZnS, the simultaneously incorporated halide ions will act as positive disturbances, and consequently these ions will give rise to empty levels below the conduction band, the empty band, which are able to trap free electrons.

Some examples of the “characteristic” type activators include Mn, Fe, and rare earth metals. Zinc sulfide with this type of activator is believed to allow electronic transitions inside of the activators (1).

Figure 4 outlines the electronic transitions that may occur in a ZnS phosphor with two different activator levels (e.g. “blue” and “green” centers) and one type of electron trap. The recombination of conduction electrons and empty activator centers is connected with fluorescence.

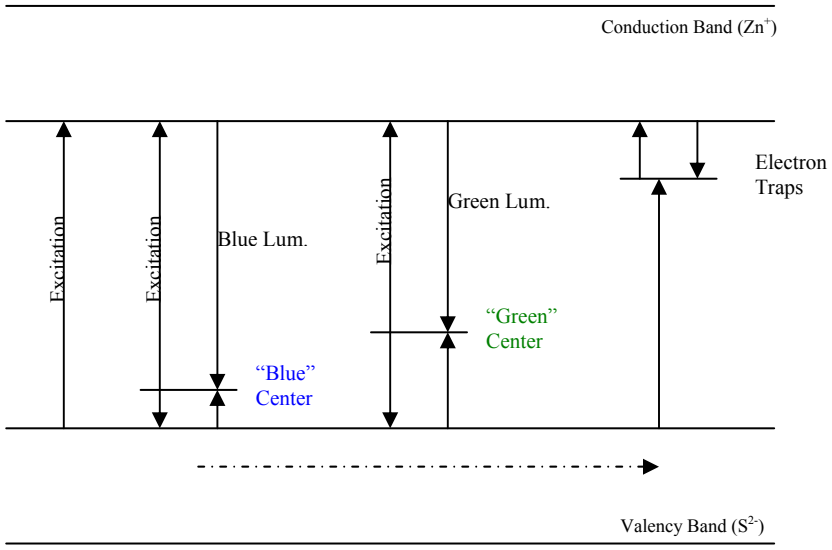

Figure 4. Energy diagrams of a ZnS phosphor, containing both blue and green luminescent centers and one type of electron trap. The solid arrows indicate electron transitions; the dotted arrow indicates hole migration (1).

The possibility of “electron” transfer between different centers may be inferred from the energy band scheme. Electrons from filled higher energy (“green”) centers will fill empty low-lying (“blue”) centers via the valence band and the emission will be predominantly green if sufficient time and activation energy is available. Holes can be defined as a vacant electron energy state that is

manifested as a charge defect in a crystalline solid, which behaves as a positive charge carrier with charge magnitude equal to that of the electron. These holes will escape more easily from the “blue” centers than from the “green” ones and can be transferred. The valence band, meaning the filled band, is the route the holes use to travel from the “blue” centers to the non-ionized “green” level (1).

TFELD

The technology of thin-film electroluminescent devices (TFELDs) has advanced rapidly in the last decade. Yellow-emitting ZnS: Mn TFELDs are now commercially available in a variety of sizes and resolutions. One example of a long-term reliable TFELD application is their use in large information boards at Helsinki Airport, which consist of 3000 EL submodules. These displays have been operating 24 hours a day since 1983. The average time it takes for failure of one submodule was calculated to be 2,000,000 hours. However, the TFELD’s are usually only guaranteed for a 40,000 hour lifetime (2).

In TFELD structures, a thin phosphor layer such as ZnS, which is sandwiched between two insulating layers, is subject to a large electric field (typically 1-3 MV cm^{-1}) when an AC voltage is applied. Due to the field emission into the conduction band from trapped interface states at these field strengths, electrons are accelerated to high enough energies to impact and excite luminescent centers, giving off visible light useful for display applications. One of the processes key to electroluminescence is the electron transport process in the

phosphor layer since light emission depends sensitively on the fraction of carriers above the threshold energy for impact excitation (2-2.6 eV) (12).

Under sufficiently low AC voltages this device behaves like a capacitor, with a loss angle (dielectric loss) on the order of 1% that varies with the frequency of the AC signal. When the electric field becomes large enough, free charges in the semiconductor layer can be transferred from one interface to the other and light emission results. The loss angle corresponds to frequency-dependent conductivity that is ascribed to some local displacement of charges. This charge transfer is usually thought to be associated with hot electrons, but also slower electrons or holes are possible (13, 14,15).

TRANSFER PHENOMENA

A complication in interpreting the intensity of the waves may arise from the interaction processes between different activator centers, which may take place if more than one type of luminescent center is present in the phosphor. If the voltage dependence of the luminous emittance, which means the giving off of light, of AC excited phosphors embedded in a dielectric medium were to deviate from that of DC excited phosphors, it would have to be ascribed to the difference in supply of the primary electrons. It has also been observed that the linear frequency dependence of the emittance may require that all available donor levels of a certain depth are exhausted as soon as the electric field surpasses a critical value, while the escape of electrons from these donors is negligible if the field strength is smaller than this critical value. This condition necessitates the

assumption of a distribution in energy of the donor levels. If all donor levels were to have the same depth below the conduction band then these donors would be field-ionized at the same critical field and, since it is assumed that the donors are localized in the interface ZnS-Cu_2S, the luminous emittance would be nearly independent of voltage (1,16).

MECHANISM OF EXCITATION

The excitation of electroluminescent zinc sulfide by an electric field gives rise either to ionization or excitation of the fluorescent centers. A calculated estimation of the field strength required for impact ionization may be obtained from the theoretical work of Von Hippel and Fröhlich on breakdown processes in ionic crystals (3). Electron avalanches induced by electrons in the conduction band of the crystal cause the dielectric breakdown of insulators according to these authors. In order to produce secondaries by impact with the ions (or atoms) of the lattice, these electrons must gain sufficient energy in the electric field (1).

FREQUENCY DEPENDENCE ON SPECTRAL DISTRIBUTION

The luminous emittance has been found for phosphors suspended in an insulating medium to increase linearly with frequency at a constant voltage over a limited range of frequencies. If an electroluminescent cell consisting of ZnS phosphor is connected in series with a capacitor, then the luminous emittance may vary superlinearly or sublinearly with frequency or may be independent of

the frequency, dependent on the magnitude of the capacitance. The actual voltage across the cell as determined by the frequency of the applied field, ω, and its amplitude is given by $\omega RCV_0 / \sqrt{(1+\omega^2 R^2 C^2)}$ in which C is the capacitance of the series capacitor, R the resistance of the cell and V_0 is the amplitude of the voltage applied to the whole system of capacitor and electroluminescent cell. Therefore, an electroluminescent cell with the ZnS grains suspended in an insulating medium can be considered as a complicated linking of parallel and series capacitors and resistors (1).

Figure 5 shows the spectral distribution of electroluminescent zinc sulfide copper aluminum and electroluminescent zinc sulfide copper chloride. The AC frequency dependence is evident in this spectral distribution of the copper-aluminum doped electroluminescent phosphor. The higher the frequency the more the blue copper band predominates. The blue: green ratio remains the same if the voltage is varied while at a constant frequency.

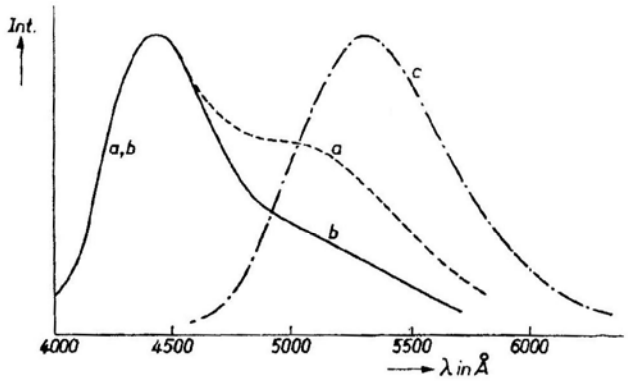

Figure 5. Spectral distribution of electroluminescent ZnS:Cu,Al at 50 c/s (a) and 500 c/s (b) and of electroluminescent ZnS:Cu,Cl phosphor at 50 and 500 c/s (c). (1)

PHYSICAL MODEL FOR IONIZATION PROCESS

After studying the methods of preparation of electroluminescent phosphors and the electrical and optical measurements, it is evident that the electroluminescence of these powders is a surface effect. According to Piper and Williams, a potential barrier at the interface between the zinc-sulfide and the copper-rich phase exists. The Fermi level of the copper-rich phase is assumed to be below that of the zinc sulfide. Electrons escape from the zinc-sulfide to the copper-rich phase when both are in contact with each other, resulting in a potential barrier. This now explains the two possibilities for electroluminescence:

(a) In the barrier region, electrons are liberated from impurity levels. These electrons are accelerated until their energy is sufficient to excite the phosphor if the local field is strong enough.

(b) The potential barrier can be penetrated by electrons from the copper-rich phase by a tunneling process and can be accelerated by the electric field into the barrier (10).

LIFETIME MEASUREMENTS OF COPPER DOPED ZINC SULFIDE

One can determine various parameters such as excited state lifetimes, trap-depths, and oscillator strengths from the study of decay curves. In the study carried out by Bhatti et. al., a nitrogen laser was used to excite the sample due to its operating wavelength in the UV region, short pulse-width, large photon flux density, and high repetition rate.

When light illuminates a crystal and is absorbed so that the electrons are raised from the valence band to the conduction band, these electrons may return to the valence band after the emission of a radiation. The probability that in time *dt*, an electron returns to the ground state with the emission of light is given by *npdt*, where *n* is the number of electrons in the excited state at time *t*, after switching off the exciting radiation, and *p* is a constant for a crystal at a given temperature.

For this decay:

$dn/dt = - pn$ Equation 1

$n = n_0 e^{-pt}$ Equation 2

$I = I_0 e^{-pt}$ Equation 3

where '*I*' is the intensity of radiation at time, *t*, and I_0, the intensity of radiation at the cut-off position. Pure exponential decays were observed in case of a single set of traps while hyperbolic decays were observed due to more than one set of traps (17).

Ivey learned that electroluminescent ZnS:Cu,Cl or ZnS:Cu,Al phosphors require, respectively, about 20 or 150 μs to decay to 50% of their initial output, about 50 or 250 μs for 37%, and roughly 200 or 900 μs for 10%. Bonch-Bruevich, Marenkov, and Johnson have observed decay times as short as 10 μs for ZnS:Cu,Cl phosphors (1). By studying various parameters of deep levels, Gavryushin reported the lifetimes of localized holes from time dependencies of ZnS:Cu as being: level 1 at 1.2 μs, level 2 at 0.5 μs, and level 3 at 3 μs (18). Johnston et. al. found that $GaN_{0.025}As/GaAs$ produced a decay time of 50 μs at

room temperature (19). Johnson suggests that the measured decay time may be influenced by the construction of the cell used for testing and by the impedance of the external circuit (1).

Excited state lifetimes, τ, with corresponding Einstein's coefficient's, A, where A = 1/τ, have been reported. Tables 2 and 3 show that all the lifetimes are in the microsecond time domain.

Phosphor	300 K			300K		
ZnS:(Cu)	τ_1 (μs)	τ_2 (μs)	τ_3 (μs)	A_1*10^4 s^{-1}	A_2*10^4 s^{-1}	A_3*10^4 s^{-1}
0.03%	23.2	5.4	2.3	4.3	18.7	44.4
0.10%	21.4	4.9	1.9	4.7	20.3	52.6
0.20%	21.1	3.8	2.0	4.7	26.7	50.5
0.30%	21.3	4.9	1.9	4.7	20.5	53.5
0.40%	20.5	3.8	1.9	4.9	26.4	52.6
ZnS:(Ag)						
0.03%	10.4	3.4	0.9	9.6	29.4	114.9
0.10%	7.6	4.7	1.5	13.2	21.2	69.0
0.20%	9.8	4.9	1.3	10.2	20.4	77.5
0.30%	8.6	4.7	1.2	11.7	21.3	82.6
0.40%	7.9	4.3	1.2	12.7	23.2	85.5

Table 2. Lifetime values (τ) and Einstein's coefficients (A) taken at 300K. (17)

Phosphor	77K			77K		
ZnS:(Cu)	τ_1 (μs)	τ_2 (μs)	τ_3 (μs)	A_1*10^4 s^{-1}	A_2*10^4 s^{-1}	A_3*10^4 s^{-1}
0.03%	13.8	3.5	0.9	7.2	28.5	113.6
0.10%	13.3	3.3	0.9	7.5	30.7	117.6
0.20%	13.4	3.2	0.8	7.4	31.1	120.5
0.30%	13.3	3.2	0.8	7.5	31.3	121.9
0.40%	13.3	3.3	0.8	7.5	30.3	120.5
ZnS:(Ag)						
0.03%	2.3	*	*	43.7	*	*
0.10%	2.3	*	*	43.7	*	*
0.20%	2.4	*	*	42.6	*	*
0.30%	2.4	*	*	41.2	*	*
0.40%	2.3	*	*	43.3	*	*

*No decay times were taken (indicating purely exponential decay)

Table 3. Lifetime values (τ) and Einstein's coefficients (A) taken at 77K. (17)

It is worth noting that the short-lived phosphorescence in these phosphors is mainly due to the presence of relatively shallow trapping states as compared to other phosphors. It was reported that the excitation of these shallow traps in these phosphors was mainly attributed to the use of high peak power output (200 kW per pulse) and short pulse-width (10 ns) of the exciting nitrogen laser source. Three exponential components in ZnS: Cu at room temperature were observed in the short-lived phosphorescence decay measurements. The smallest of the

three calculated lifetimes is interpreted to be due to the transition in nearest neighbor coupled pairs while the longest lifetime is explained as due to the less effective coupling between the radical ions and their nearest neighbors. Zalm claims that when the temperature of the phosphor is lowered to liquid nitrogen level, all the lifetime values are reduced in magnitude. The investigations carried out with variable concentrations of the dopants show that the slowest component of lifetime decreases with the increase in the amount of dopant radical (1).

TIME EVOLUTION OF ELECTROLUMINESCENCE

The location of the electrons in the phosphor particle is dependent on time. The greater the voltage change, the more movement of electrons there is. Figure 6 shows the dependence on time.

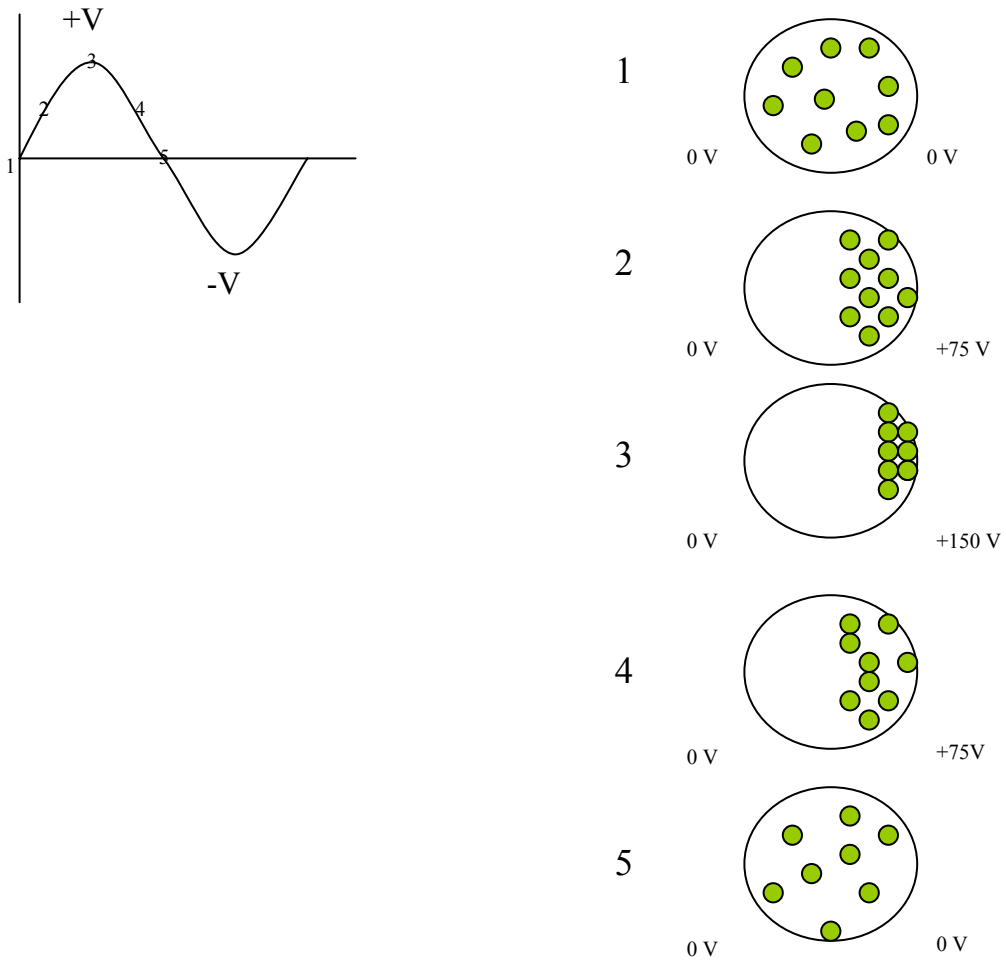

Figure 6. This illustrates the movement of electrons relative to time as a function of voltage.

CHAPTER II

Experimental

The samples that were investigated in this project were electroluminescent panels developed by Meadow River Enterprises. Each sample was 4" X 1" in size using Sylvania Type 729 Phosphor Luminescent Material. The phosphor particles are typically 20 to 50 μm. This material is ZnS:Cu used for applications such as electroluminescent lamps. The typical optical properties are as follows:

Electroluminescent at 400 Hz, 100 V (OSi Test Lamp)

Fluorescence……..Green

Wavelength at Peak, nm……504

Line Band Width (50%) nm……..76

CIE Color Coordinates……..x=0.182

y=0.455

Light Output, od/m^2……...24 hrs = 110

100 hrs = 93

The typical physical properties are as follows:

Particle Size Distribution- Coulter Counter (Size in Micrometers at Listed Percentages)

	25%	50%	75%
Spatulated Dispersion	23	29	35

Bulk Density, g/cc……1.94

Body Color……Light Green

Body Size, μm……..50

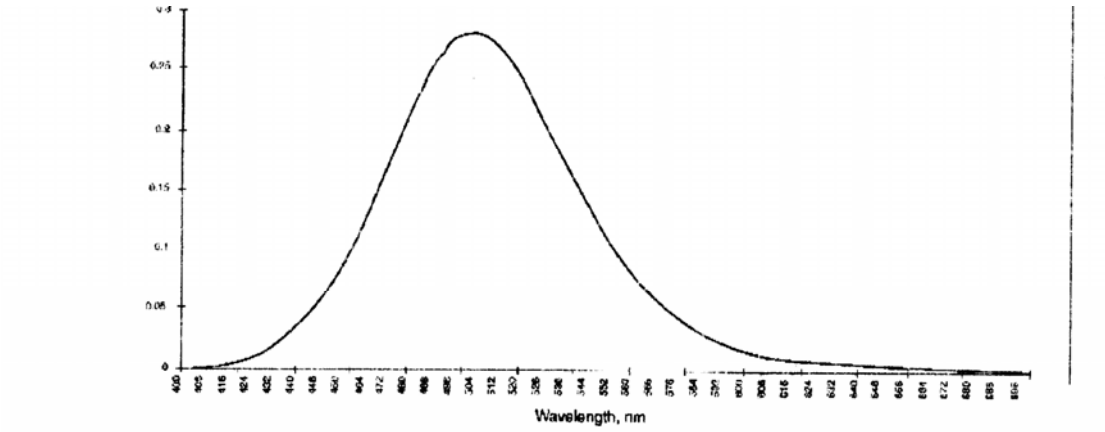

Figure 7. Typical Emission Spectra for 400 Hz 100 V (20)

The electroluminescent panels were designed to act as a capacitor. Figure 8 shows the generalized design. The dielectric layer prevents electrons from traveling long distances (such as to the SnO).

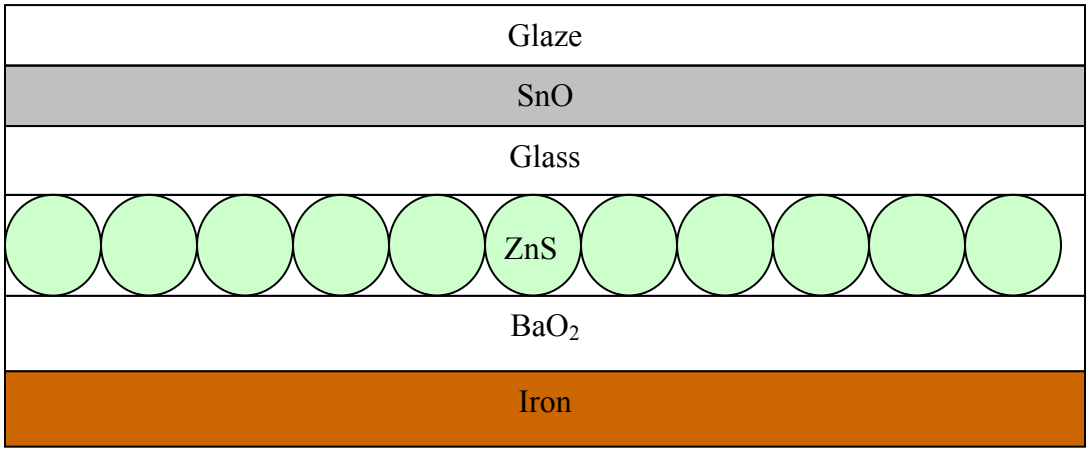

Figure 8. The electroluminescent panel design.

The apparatus designed to operate as a power supply was built by using ordinary equipment purchased from Radio Shack. A Radio Shack power supply was used in series with a signal generator. This line is then fed into an Optimus XL-200 Bridgeable Amplifier, which then connects to the Radio Shack step up transformer. This supplies the power to the electroluminescent panel.

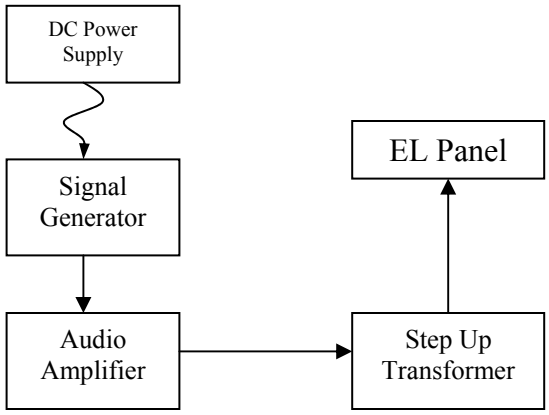

Figure 9. Diagram of set-up used to power panels.

CHAPTER III

Results and Discussion

It is apparent to the unaided eye that the emittance of the manufactured electroluminescent panels varied in color according to the frequency of AC electrical excitation. In general, the higher the frequency, the bluer the emittance color of the panel. Lower frequencies caused the panel to emit a green color. Therefore, a study was designed to analyze the relationship between AC frequency and the emittance color.

Three frequencies were selected for the investigation. Data was taken for 200 Hz, 1500 Hz, and 20 kHz. The following figures present intensity data which were obtained by measuring the voltage output of a photomultiplier tube (Oriel Model 70680) while varying the wavelength passed by a monochromator (Oriel Model 77200) at a constant AC excitation frequency. This process was repeated at each of the three standard excitation frequencies. Figure 10 shows the spectrometer setup that was used to collect the data.

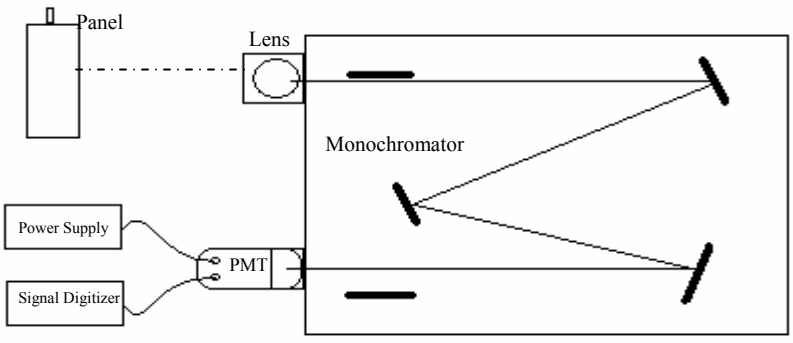

Figure 10. The spectrophotometer setup used to collect data.

The output voltage of the photomultiplier tube is proportional to the intensity of the lamp. As the excitation frequency of the panel was changed, the output voltage of the PMT also rises from the increased intensity. For each frequency, the intensity was recorded from the wavelengths 300 nm to 700 nm while the AC voltage was kept constant at 100 V.

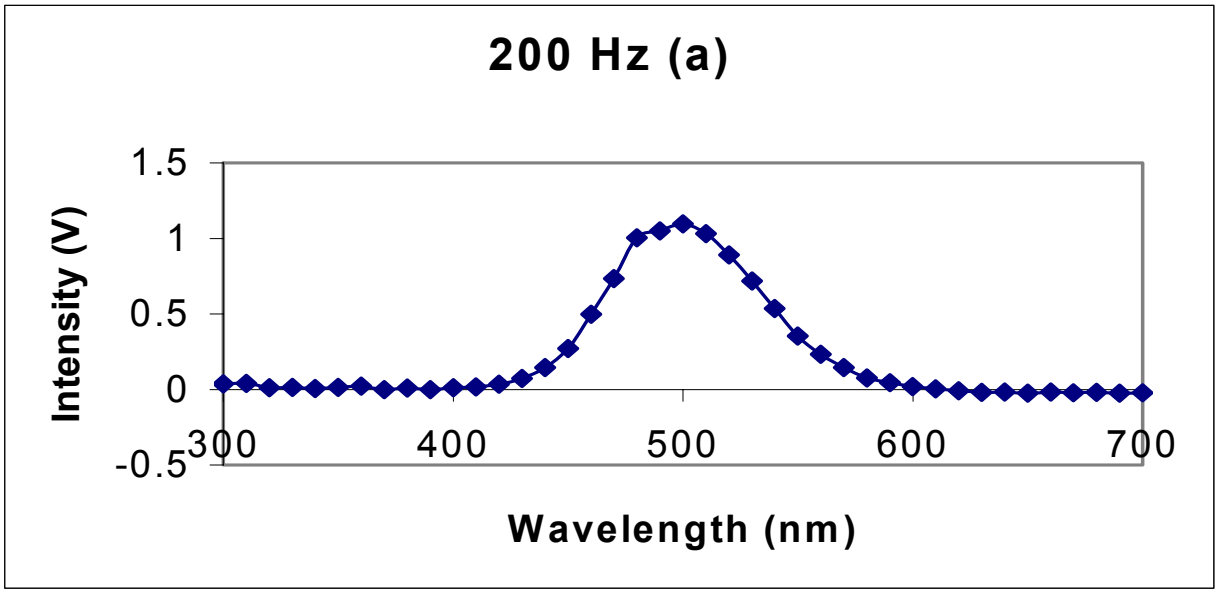

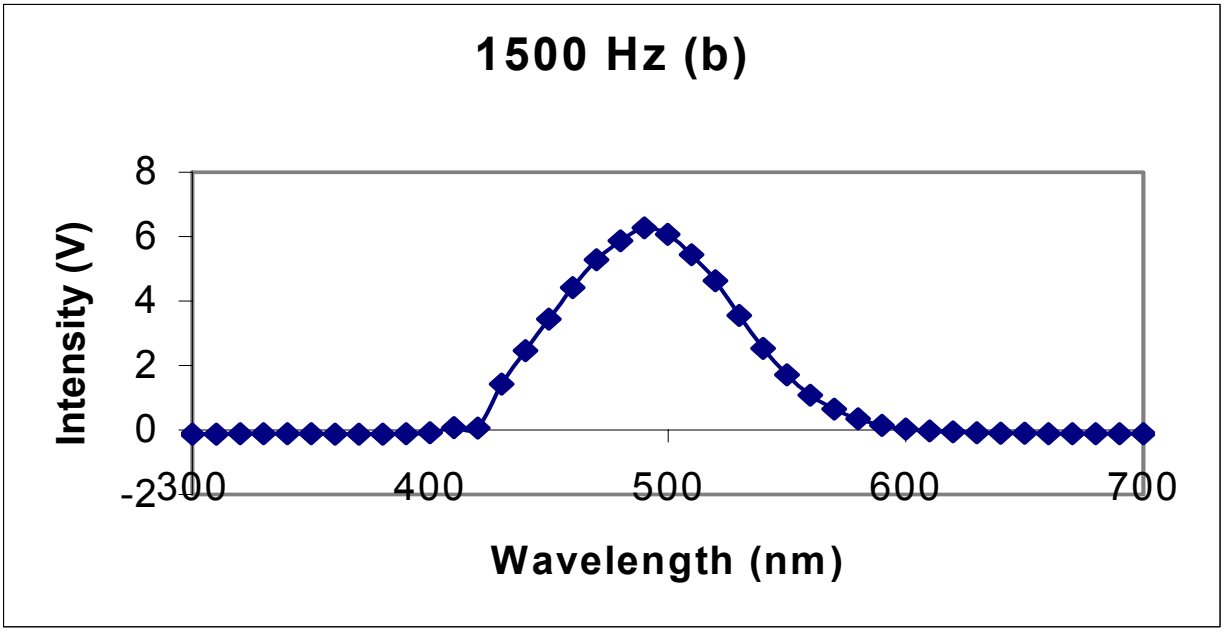

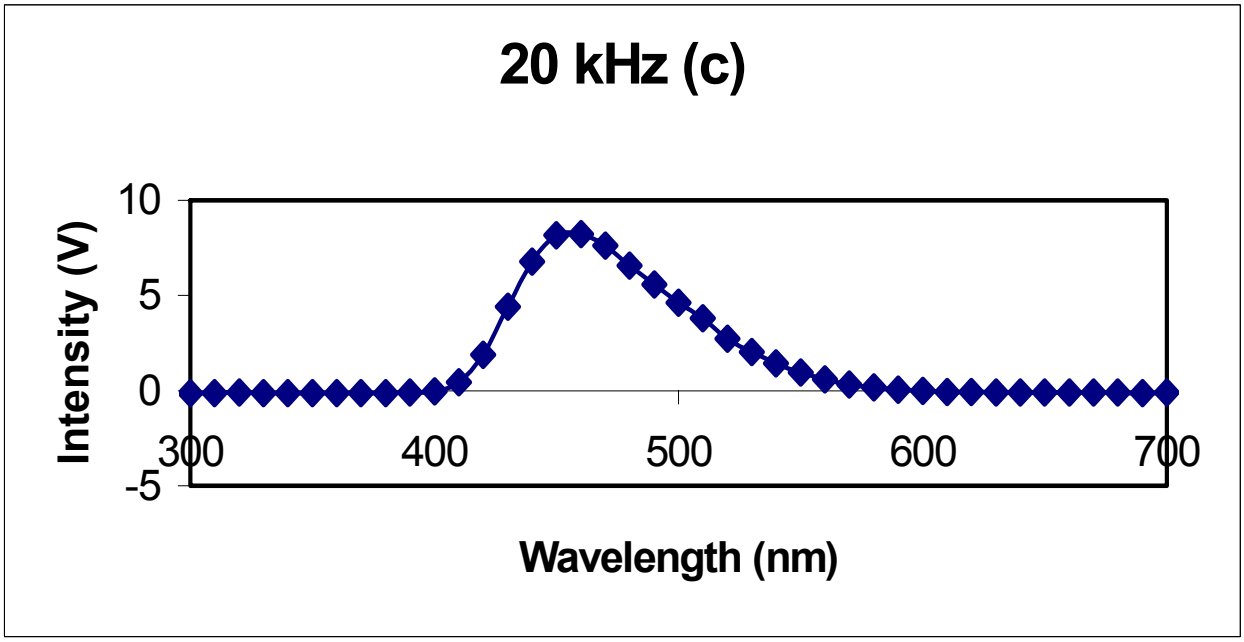

Figures 11a-11c. 11a) (top) Diagram of 200 Hz Emission Spectra. 11b) (middle) Diagram of 1500 Hz Emission Spectra. 11c) (bottom) Diagram of 20 kHz Emission Spectra.

Figures 11a-11c indicate the emission spectra of the various frequencies chosen. Figure 11a is the data for the 200 Hz excitation taken at a constant voltage of 100 volts. It can be seen that the maximum intensity reached is 1.095 volts at 500 nm. Figure 10b shows the emission spectra collected at 1500 Hz yielding a maximum intensity of 6.276 volts at 490 nm. Figure 10c indicates the chart of the 20 kHz data producing a maximum intensity of 8.215 volts at 460 nm. Therefore it can be concluded that as the frequency increases, the wavelength associated with the emission intensity maximum decreases. At each frequency the emission intensity was observed to increase, non-linearly with frequency.

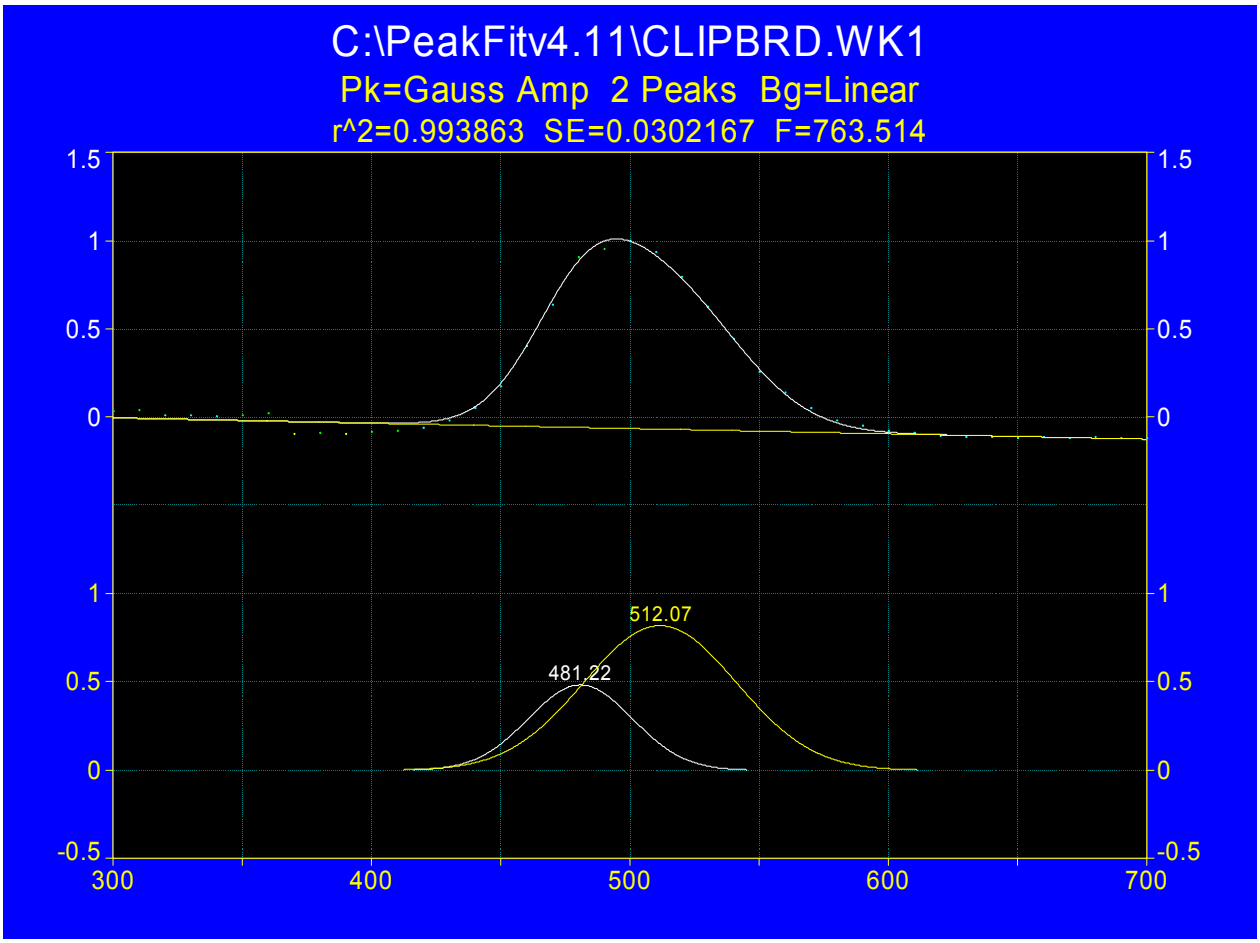

Figure 12. A double gaussian fit for the 200 Hz emission spectra using peakfit. The two overlapping peaks are separated at the bottom.

The complete emission spectrum is shown in Figure 12 on the top. This data is the same as Figure 11a. A gaussian fit algorithm was used to then resolve the peak into two overlapping gaussian curves. The maxima were then determined to be at 481 nm and 512 nm. Further analysis utilizes these wavelengths as the approximate values: 480 nm and 515 nm.

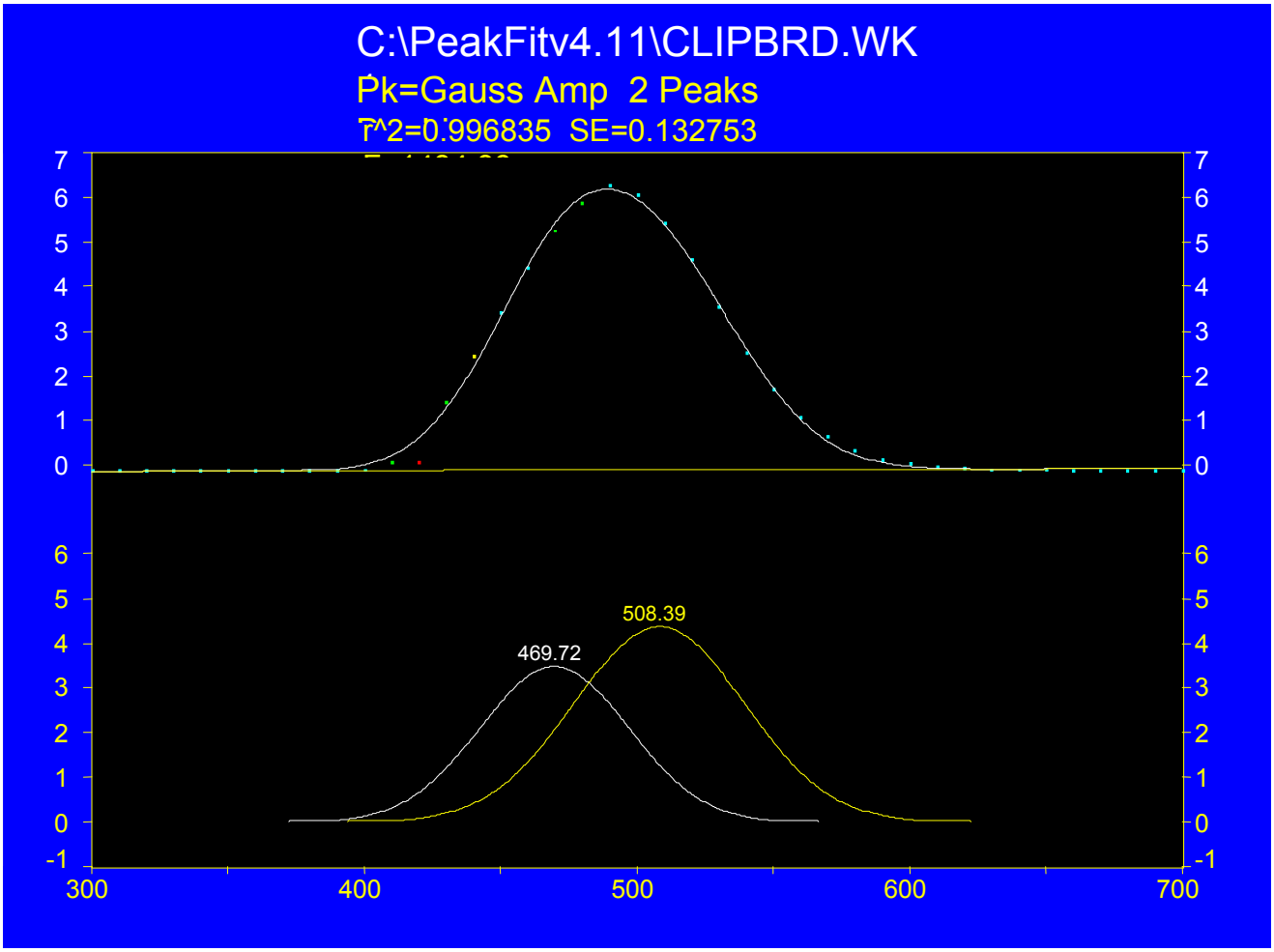

Figure 13. A gaussian curve for the 1500 Hz emission spectra using peakfit.

By looking at Figure 13, the emission spectrum of 1500 Hz can be seen. The original data is shown in Figure 11b. The Gaussian deconvolution program was used to resolve the emission spectrum into its two component curves. These emission processes are determined to have their maximum intensities at 469 nm and 508 nm. The approximate values used in further investigations are: 470 nm and 510 nm.

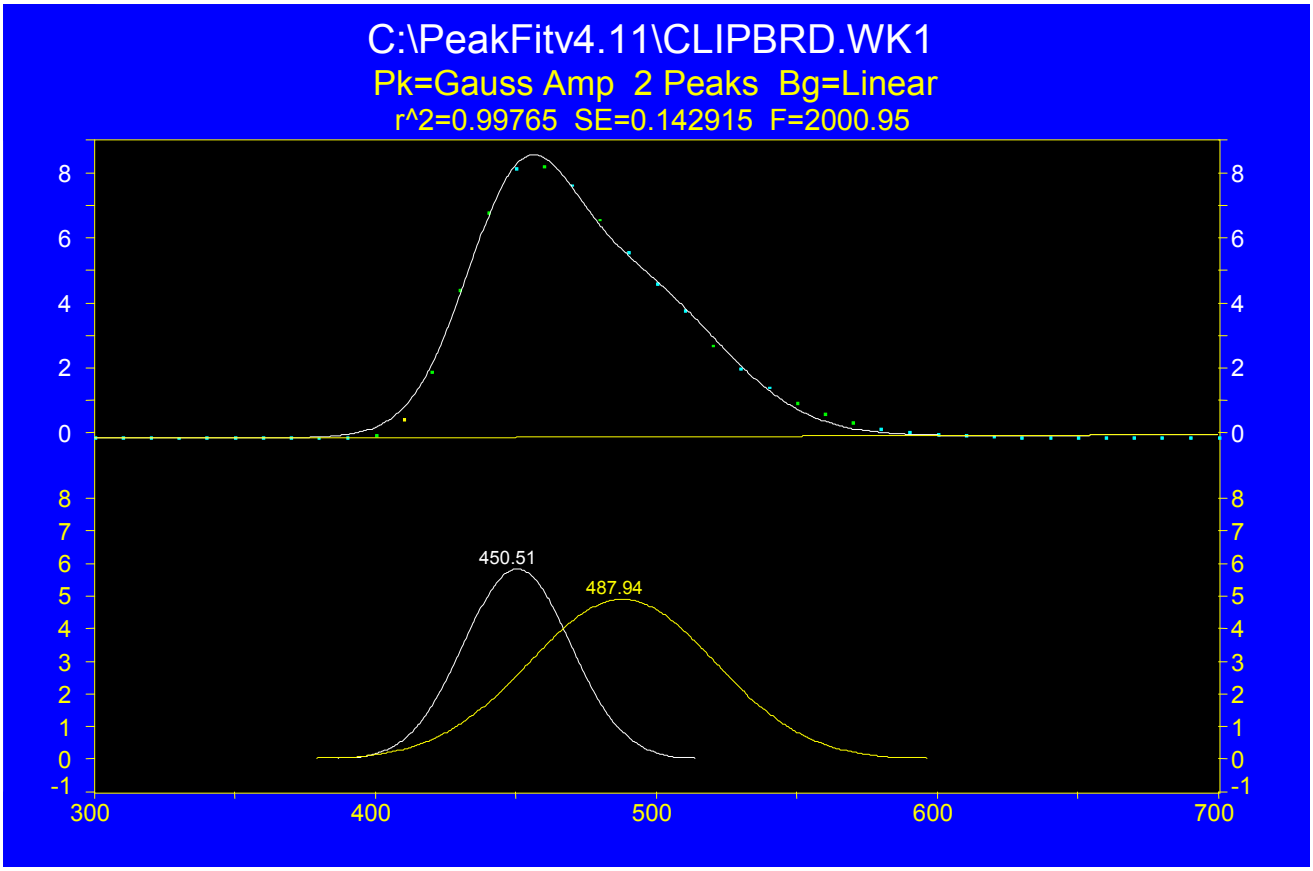

Figure 14. A gaussian curve of the 20 kHz emission spectra using peak fit.

The emission spectrum for the 20 kHz excitation frequency is shown in Figure 14. The data was taken from the original spectrum, as seen in Figure 11c. Using a Gaussian fit program, the overlapping curves were separated out to yield gaussians with maxima at 450 nm and 487 nm or 450 nm and 488 nm.

The Peakfit software program was used to deconvolute the observed spectrum into two Gaussian distributions. The two emission envelopes can then be characterized by the wavelengths of maximum emission for each frequency:

200 Hz	→	481 nm	512 nm
1500 Hz	→	470 nm	510 nm
20 kHz	→	450 nm	488 nm

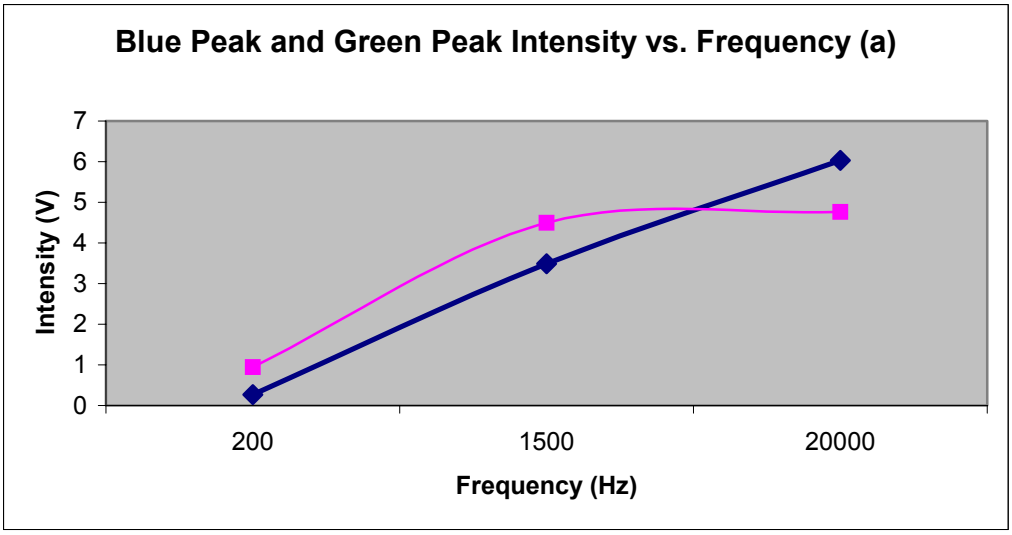

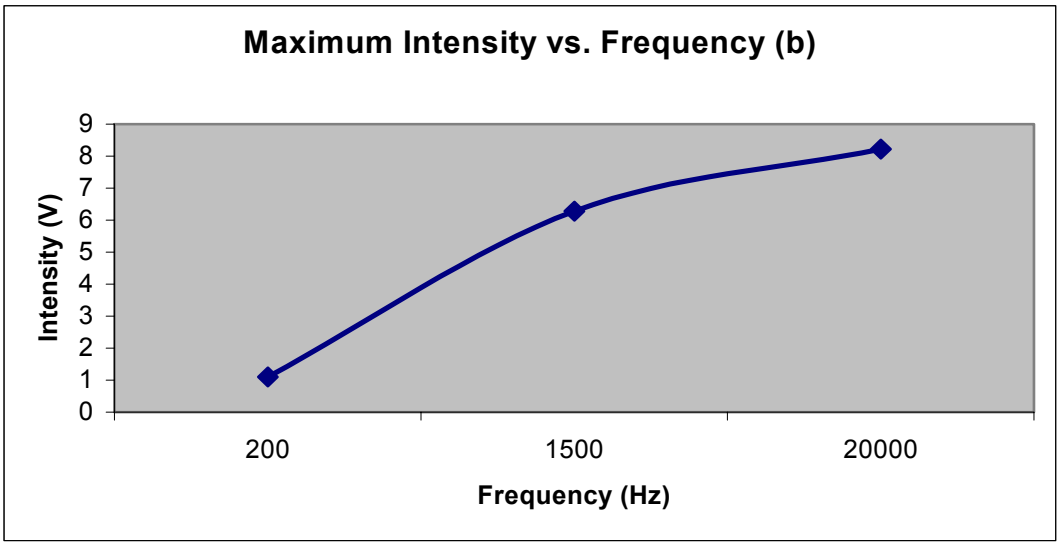

Figure 15a. Diagram of peak 1 (blue) intensity and peak 2 (green) versus frequency. 15b) Diagram of maximum intensities versus frequency.

Using the data from Figures 12, 13, and 14, the Figures 15a and 15b were produced. The intensity of peak 1 (the "blue" peak) in each diagram was plotted along with the frequency in Figure 15a. Figure 15a also has the plot of the

intensity of peak 2 (the “green” peak) versus frequency. Finally, the graph in Figure 15b represents the maximum intensities, of the original emission spectra, versus the AC frequency.

By looking at these individual graphs, it is observed that the “blue” peak intensity increases almost linearly with frequency. However, the “green” peak becomes saturated, i.e. the increase of intensity levels off. An explanation for the saturation of the “green” peak can only be speculated. In order to investigate this saturation phenomena in more detail, a series of time dependent experiments was performed.

FREQUENCY	BLUE FWHM	GREEN FWHM
200 Hz	47.80	65.47
1500 Hz	62.19	75.25
20 kHz	44.92	77.92

Table 4. Table indicating the full width – half-max of the blue peak and the green peak at the three observed AC excitation frequencies.

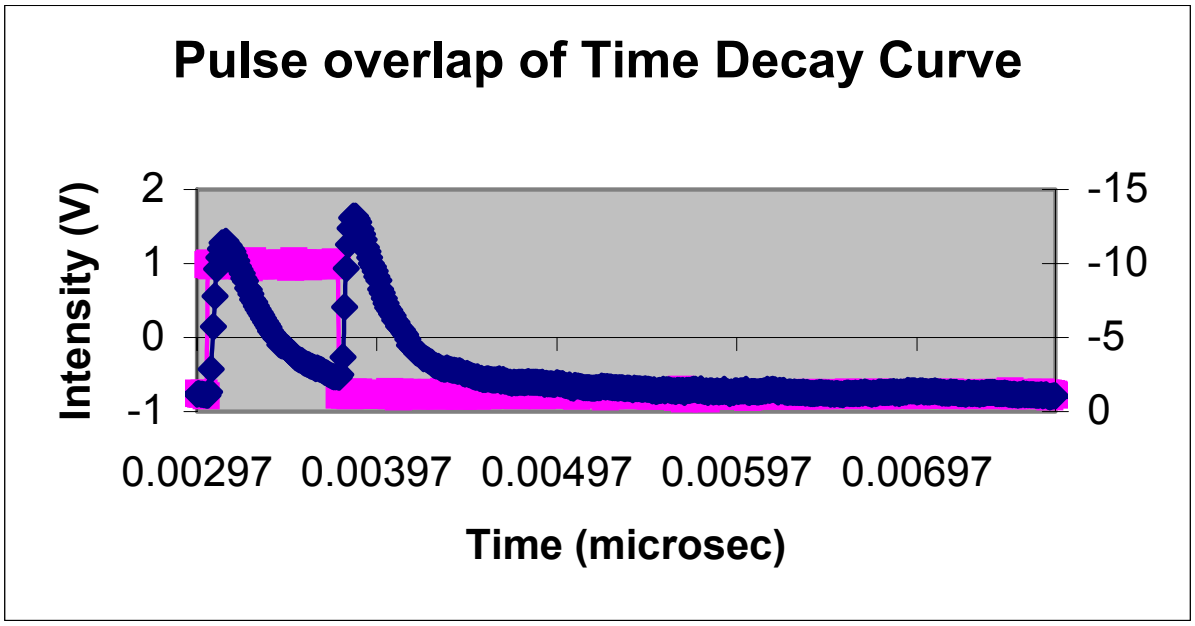

Figure 16. A graph detailing the overlap of the optical pulse waveform (blue) on the excitation waveform (pink).

DECAY CURVES

A pulse system was used to excite the EL Panel at the designated frequencies. Figure 16 illustrates the pulse overlap of a time decay curve at 200 Hz. Light is emitted only when there is a change in potential, as can be seen in Figure 16. A square waveform was pulsed, while the emittance was recorded simultaneously. The emittance is measured as the output voltage of the PMT. This output voltage is directly proportional to the emission intensity of the EL panel. The maximum emittance is reached as the waveform has a change in potential.

Figures 17, 19, 21, and 23 are the diagrams showing the oscilloscope views of the 200 Hz 480 nm, 200 Hz 515 nm, 1500 Hz 470 nm, and 1500 Hz 510 nm pulse overlaps of the electroluminescent panels respectively. If comparing the 200 Hz 480 nm view to the 200 Hz 515 nm view, it can be seen that the 515

nm pulse has two peaks equivalent in intensity. However, the 480 nm pulse shows the second peak has an increased intensity in comparison with the 515 nm view.

Also, if looking at the 1500 Hz 470 nm view and the 1500 Hz 510 nm view, the difference is apparent. The second peak of the 470 nm curve is considerably more intense than the second peak. While the 510 nm pulse shows the second peak being only slightly more intense than the first peak.

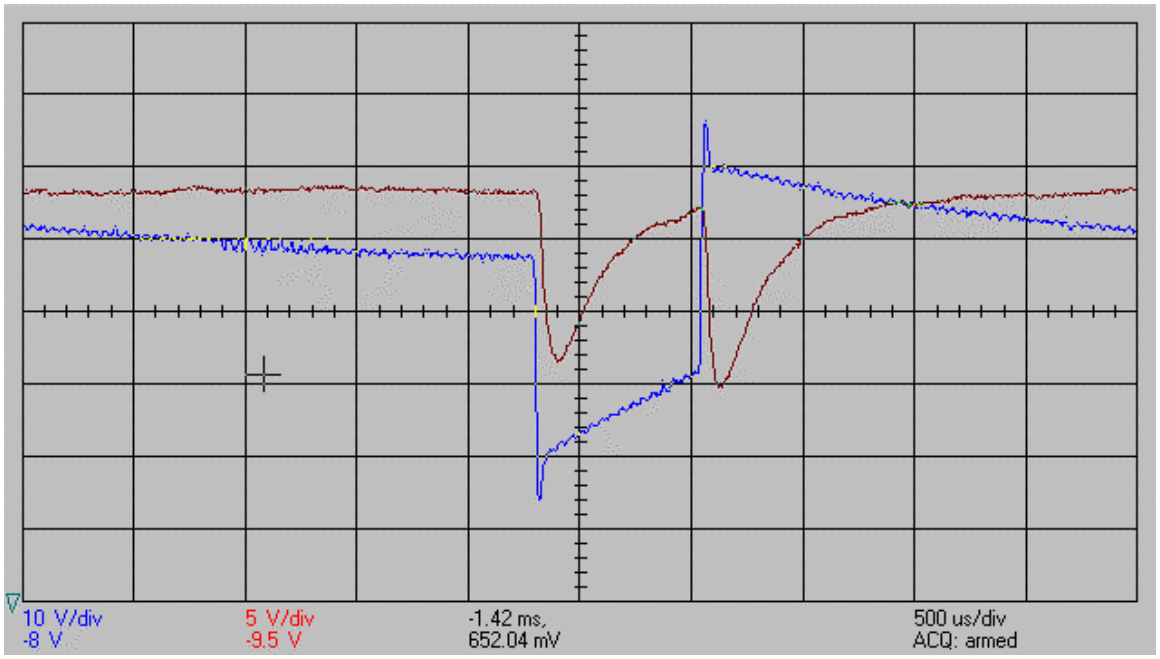

Figure 17. The oscilloscope view of the pulse overlap of the electroluminescent panel at 200 Hz, 480 nm.

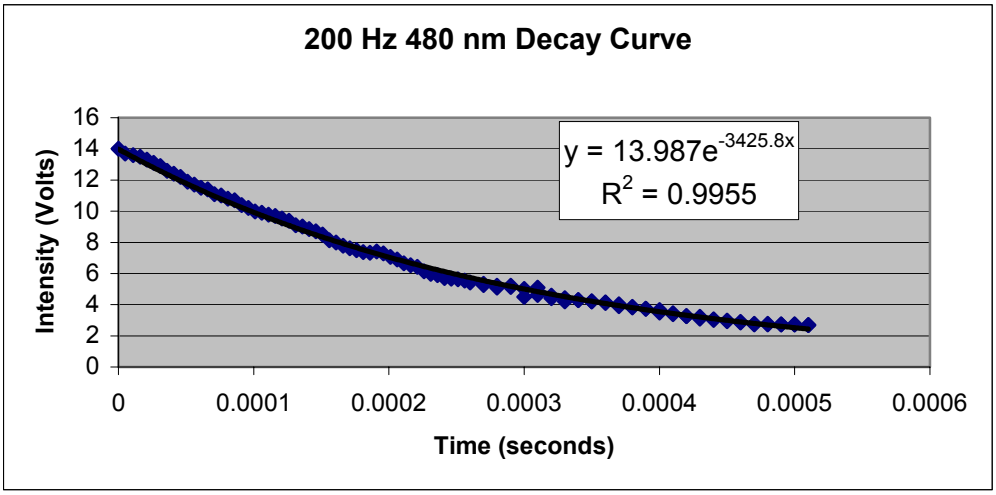

Figure 18. The decay curve of the electroluminescent panel excited at 200 Hz, 480 nm.

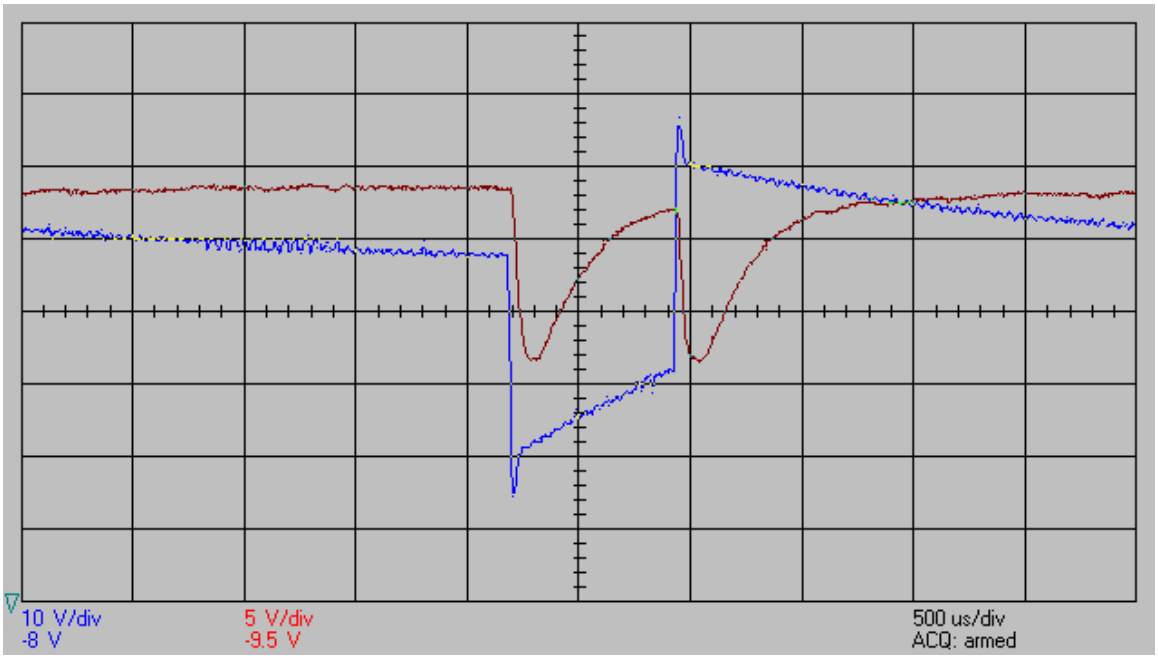

Figure 19. The oscilloscope view of the pulse overlap of the electroluminescent panel at 200 Hz, 515 nm.

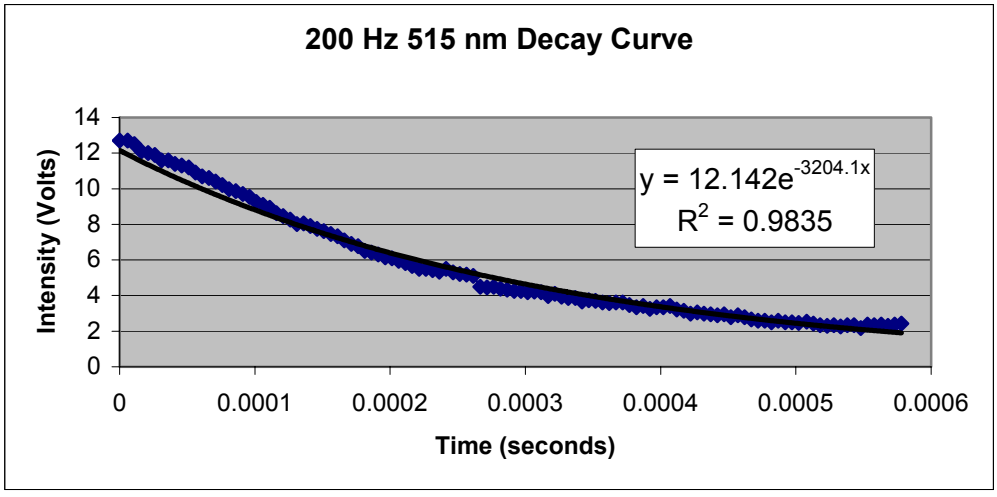

Figure 20. The decay curve of the electroluminescent panel excited at 200 Hz, 515 nm.

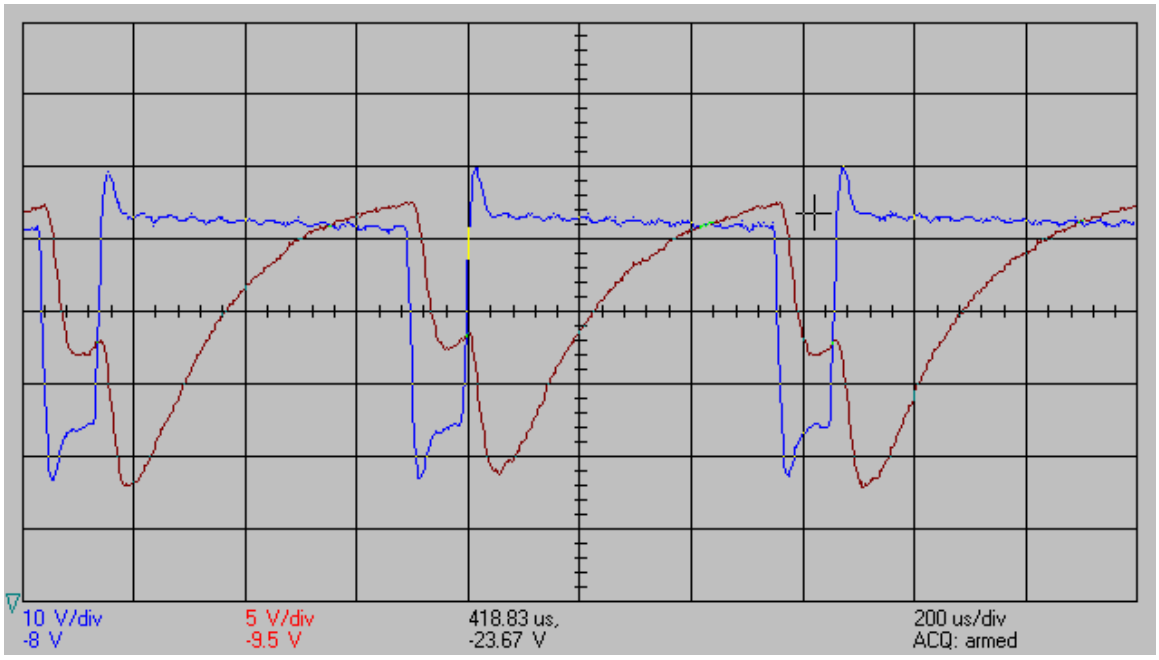

Figure 21. The oscilloscope view of the pulse overlap of the electroluminescent panel at 1500 Hz, 470 nm.

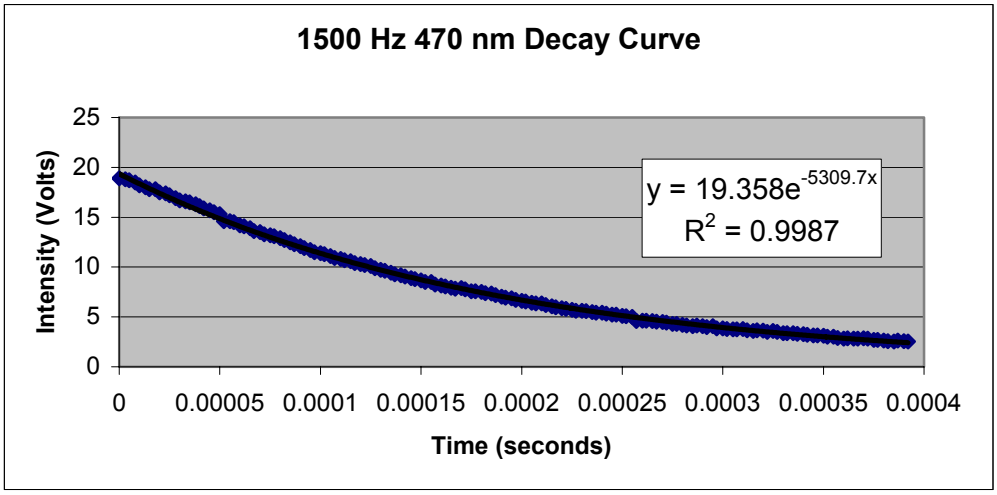

Figure 22. The decay curve of the electroluminescent panel excited at 1500 Hz, 470 nm.

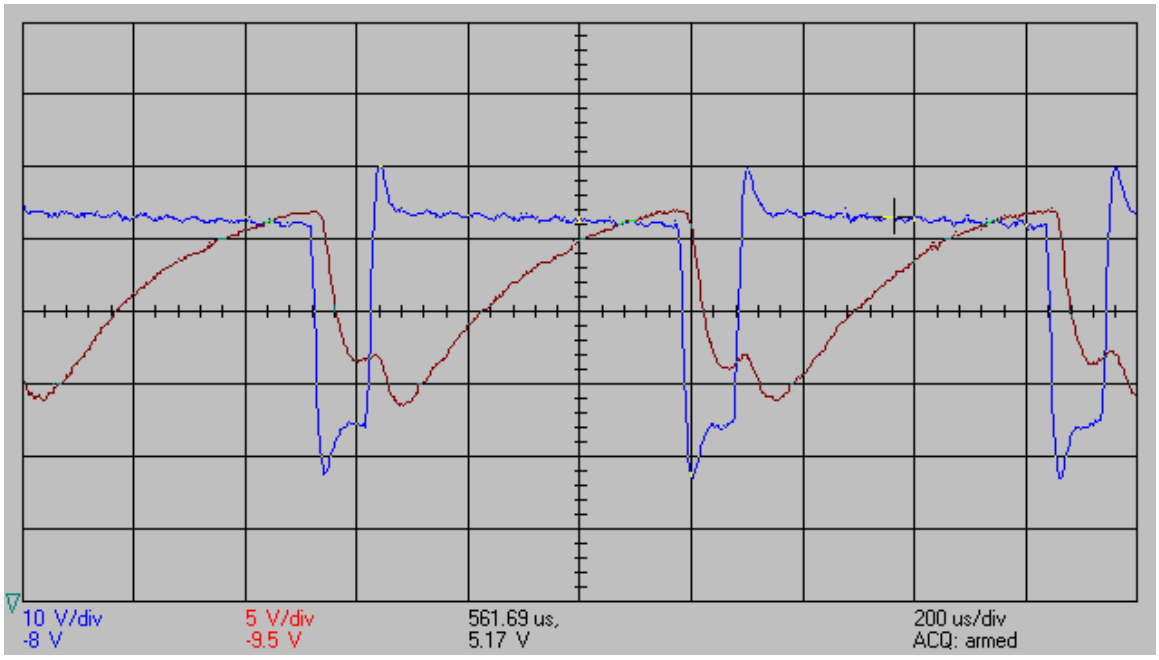

Figure 23. The oscilloscope view of the pulse overlap of the electroluminescent panel at 1500 Hz, 510 nm.

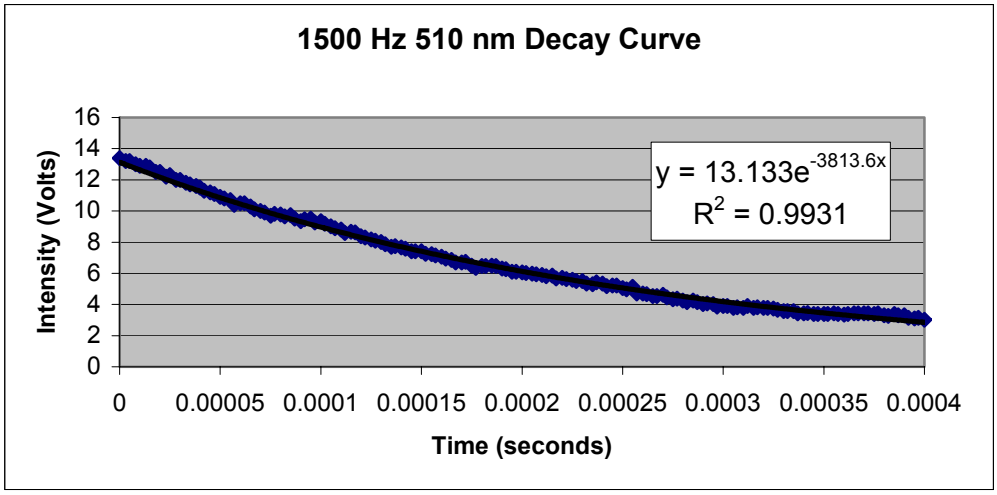

Figure 24. The decay curve of the electroluminescent panel excited at 1500 Hz, 510 nm.

Pulse Experiment	Maximum Intensity of Pre-pulse (V)	Baseline Intensity (V)	Maximum Intensity of Pulse (V)	Ratio
200 Hz, 480 nm	-12.3	-0.54	-14.9	1.22
200 Hz, 515 nm	-13.3	-1.06	-13.2	0.99
1500 Hz, 470 nm	-12.5	-2.34	-21.8	1.91
1500 Hz, 510 nm	-14.0	-2.66	-16.1	1.18

Table 5. Table containing data that is crucial to the Decay Curves. This data includes the maximum intensity of the pre-pulse excitation, the maximum intensity of the pulse, and the intensity at the baseline (right before the pre-pulse). The ratio was then calculated by the following equation 4 below.

Table 5 summarizes the data observed in Figures 16-23. The values for the various intensities shown are approximate, since the baseline value (where the decay curves cease) was estimated. The ratio was calculated using the following equation:

$$\text{Ratio} = \frac{(\text{Maximum Pulse}) - (\text{Baseline Intensity})}{(\text{Maximum Pre-Pulse}) - (\text{Baseline Intensity})} \qquad \text{Equation 4}$$

This ratio is essentially the fraction of excess light emitted during the pulse compared to the light emitted during the pre-pulse. By comparing the ratios, it can be observed that the blue emissions at each frequency are considerably higher than the green emissions. It can also be seen that as the AC frequency increases, the ratio increases as well. The blue pulse has higher intensities at both AC excitation frequencies than the green. This must be due to the location

of the relative location of these energy states and the electronic structure of the phosphor. It would appear that a non-saturable reservoir of electrons is exists and is populated by the ionization process for the blue emission, resulting in there being more electrons available to fill the blue levels. Thus, the intensity of the blue emission is greater than the green intensity.

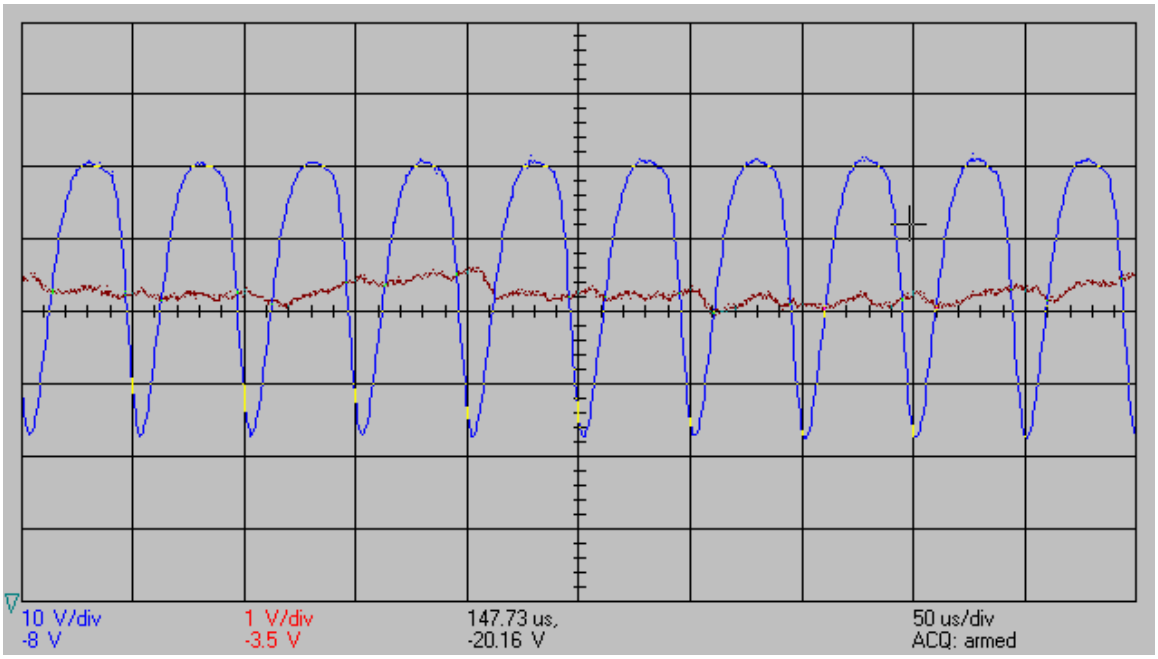

Figure 25. The oscilloscope view of the pulse overlap of the electroluminescent panel at 20 kHz, 450 nm.

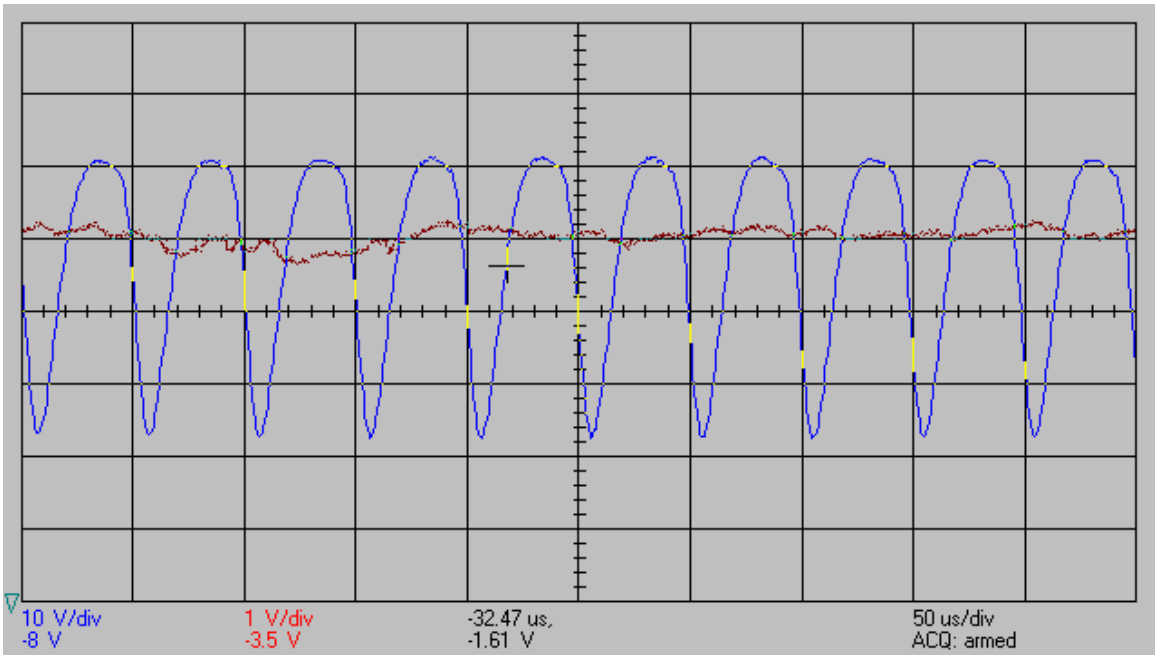

Figure 26. The oscilloscope view of the pulse overlap of the electroluminescent panel at 20 kHz, 488 nm.

Figure 25 shows the oscilloscope trace of the pulse overlap recorded at 20 kHz, 450 nm, while Figure 26 shows the view of the pulse overlap taken at 20 kHz, 488 nm. An actual pulse waveform cannot be observed due to the high frequency. The frequency is so high that there is not enough time to allow the excitation from the pre-pulse to drop back down before the next excitation pulse. For this reason, a decay curve could not be extracted from the pulse waveform.

The lifetime was calculated for the following decay curves: 200 Hz 480 nm, 200 Hz 515 nm, 1500 Hz 470 nm, and 1500 Hz 510 nm. In order to resolve the lifetime, the rate constant had to be determined. This was carried out by fitting an exponential trend line to each decay curve. The exponential decay equation is as follows:

$$N(t) = N_0 e^{-kt} \qquad \text{Equation 5}$$

where N_0 is the original number of atoms, k is the decay constant, and t is the time. Equation 5 is otherwise known as the law of radioactive decay. The decay constant can then be related to the lifetime by the following:

$$t_{½} = \frac{0.693}{k} \qquad \text{Equation 6}$$

Using this method of calculation, the lifetime values were determined and are presented in Table 6.

Pulse Decay Curve	Lifetime (μs)
200 Hz, 480 nm	202.3
200 Hz, 515 nm	216.3
1500 Hz, 470 nm	130.5
1500 Hz, 510 nm	181.7

Table 6. The lifetimes of the blue emissions and green emissions as calculated using the law of exponential decay.

CHAPTER IV

Conclusion

After reviewing other models for the electronic structure of Cu doped ZnS, an explanation for the frequency dependence of the color of emission is suggested. Figure 27 shows the electron paths for the blue emission and the green emission. Electrons are initially excited from a variety of states, including the valence band up to the conduction band through a variety of ionization processes. Some of these electrons then fall into the intermediate state. If the electron falls into the intermediate state and then to the “e” state, then blue light is emitted. However, if the electron falls from the conduction band directly to the t_2 -state, then green light is emitted. The blue emission is therefore a two step process, in which the intermediate state can act as a carrier reservoir, while the green emission is only a one step process, where the conduction band must provide the charge reservoir. The explanation for the observation that higher frequency AC excitation yields a bluer color may depend on differences in population of the conduction band versus population of the intermediate state. It would appear that the population of electrons in the conduction band, which can contribute to luminescence, is saturable (limited), since the intensity of the green emission seems to be limited. In contrast, the number of intermediate electronic states that can be occupied and give rise to the blue emission appears to be greater than the number of conduction band states. With each additional AC transient, the population of the intermediate state appears to grow. We arrive at this conclusion by comparing the Blue to the Green emission intensities in the

second pulse at both low and intermediate frequency AC excitation. In each case, the rise in blue emission is greater than the rise in green emission. Each re-excitation of electrons in the conduction band puts in carriers which can decay through multiple modes, and does not appear to add extra electrons capable of producing green luminescence. In contrast, each pulse adds additional species capable of yielding blue emission. At low frequency, both conduction and intermediate states can empty before the next pulse (AC transient) arrives. This yields a baseline ratio of blue to green photons. It would be anticipated that below a certain frequency, little color change would be anticipated. At high frequencies, the pulses add to the population of the intermediate state, but do not raise the population in the conduction band. Another prediction from this model would be that beyond a certain frequency, no change in relative intensity (blue vs. green) would be observed. The lifetime of either of these states cannot be determined, only the radiative lifetimes can be determined, and those are shown in Table 6. The differences in lifetimes and FWHM for the two different processes (blue emission process and green emission process) are consistent with the attribution of different final and initial states provided in Figure 27. The relative changes in both of these parameters with frequency (from Table 4, blue lifetime changes by 23% and green lifetime changes by 13% on going from 200 Hz to 1500 Hz, while from Table 5, the FWHM for the blue emission changes by 36% and the green emission peak shape changes by 16% with the same change in AC frequency).

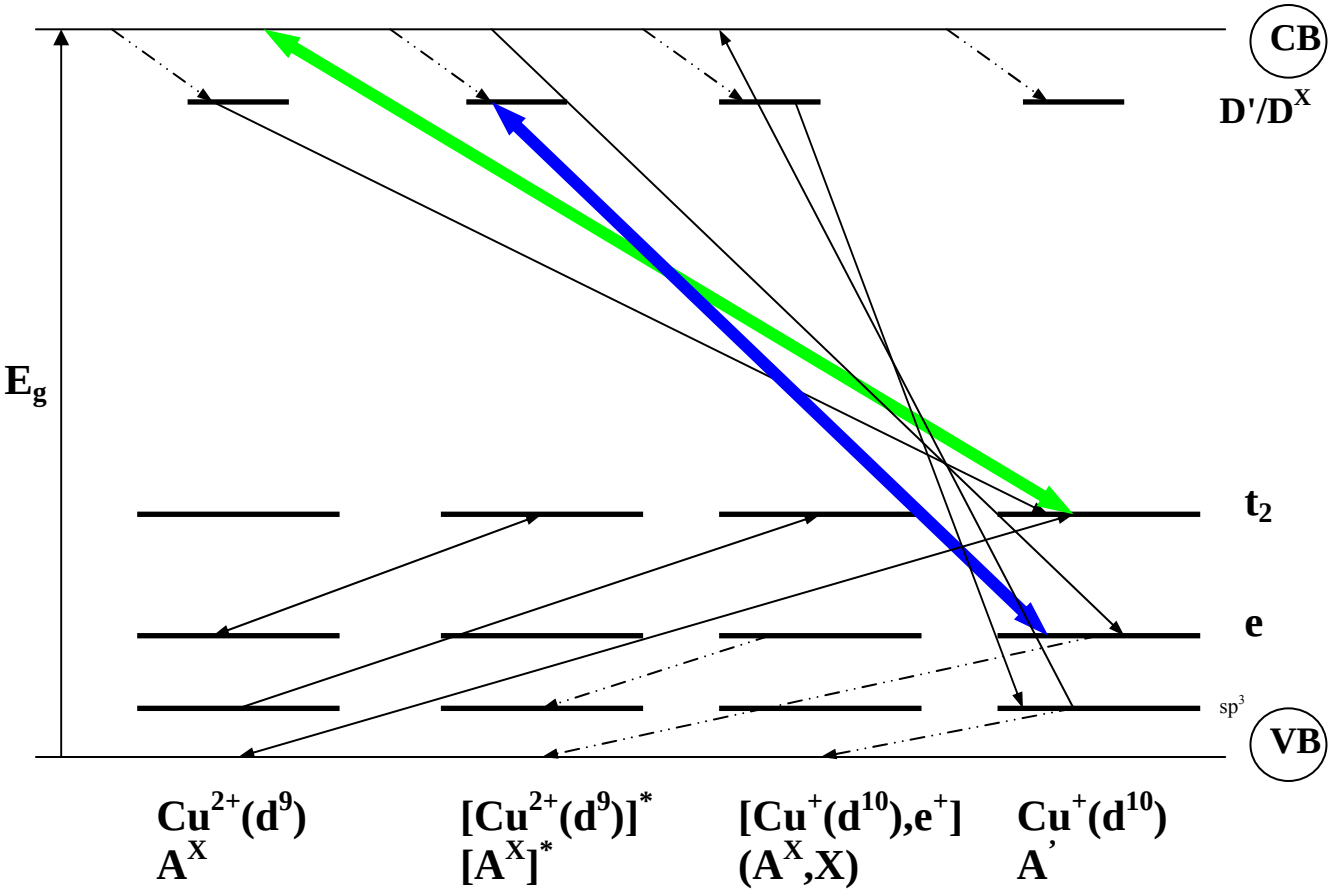

Figure 27. Energy levels of Cu, indicating the blue and green emissions. The blue line represents the electron path for the blue emission, while the green line indicates the electron path for the green emission (8).

CHAPTER V

FUTURE WORK

Future work on this intriguing project is recommended. Future projects may broaden the variables investigated to include: varying temperatures, photoconductivity studies, photoluminescence studies, photoluminescent lifetime studies, different firing temperatures, different types, concentrations and combinations of dopants, and an assortment of panels. With technology continually advancing, it is highly likely that this product could easily be utilized for street signs, helicopter landing pads, license plates, etc.

REFERENCES

1. Zalm, P. "The Electroluminescence of ZnS Type Phosphors." *Philips Research Reports.* 11, 353-451, 1956.
2. Gumlich, H.-E., A. Zeinert, and R. Mauch. Luminesence : Electroluminescence. Plenum Press: New York, 1998.
3. Ivey, Henry F. Electroluminescence and Related Effects. Academic Press: New York, 1963.
4. Arterton, B., J.W. Brightwell, S. Mason, B. Ray, and I.V.F. Viney. "Impact of Phase Concentrations on Structure and Electroluminescence of ZnS:Cu." *Journal of Crystal Growth*. 117, 1008-1011, 1992.
5. Bellotti, E., K.F. Brennen, R. Wang, and P.P. Ruden. "Monte Carlo Study of Electron Initiated Impact Ionization in Bulk Zincblende and Wurtzite Phase ZnS." *Journal of Applied Physics*. 83(9), 4765-4772, 1998.
6. www.chemistry.ohio-state.edu/~woodward/ch754/struct/ZnS.htm
7. www.chemistry.ohio-state.edu/~woodward/ch754/struct/ZnO.htm
8. Peka, P. and H.-J. Schulz. "Empirical One-Electron Model of Optical Transitions in Cu-Doped ZnS and CdS." *Physica B*. 193, 57-85, 1994.
9. Ohta, Shin-ichi, Toyoyasu Tadokoro, Shuji Satou, Satoshi Kobayashi, and Futao Kaneko. "Effects of Mn Effusion Cell Temperature on the Film

Properties and on the AC Electroluminescence of Molecular Beam Deposited ZnS:Mn." *Journal of Luminescence.* 47, 41-47, 1990.

10. Zalm, P., G. Diemer, and H.A. Klasens. "Electroluminescent ZnS Phosphors." *Philips Research Reports*. 9, 81-108, 1954.
11. Khomchenko, V., V. Rodinov, L. Zavyalova, G. Svechnikov, N. Roshchina, V. Khachatryan, A. Savin, Yu Bacherikov, O. Marchilo, Yu Tzyrkunov, and J. Stiles. "Electroluminescent ZnS-Cu Films Made by Metal-Organic Chemical Vapour Deposition and Thermodiffusion." *Semiconductor Science Technology*. 18, 512-516, 2003.
12. Hui, Zhao, Wang Yonsheng, Xu Zheng, and Xu Xurong. "Transient Acceleration Process of Electrons in ZnS-type Thin Film Electroluminescence Devices." *Journal of Physics; Condensed Matter*. 11, 2145-2151, 1999.
13. Gupta, S., J.C. McClure, and V.P. Singh. "Phosphor Efficiency and Deposition Temperature in ZnS:Mn A.C. Thin Film Electroluminescence Display Devices." *Thin solid Films*. 299, 33-37, 1996.
14. Neyts, K.A., and P. DeVisschere. "How to Measure and Interpret the Conduction Current in AC Thin-Film Electroluminescent Devices." *Solid State Electronics*. 35:7, 933-936, 1992.
15. Neyts, Kristiaan and Dorina Corlatan. "UV-Induced Charge Transfer and Light Emission in ZnS-Based Electroluminescent Devices with Probe Layer." *Physica B*. 193, 57-65, 1993.

16. Zalm, P., G. Diemer, and H.A. Klasens. "Some Aspects of the Voltage and Frequency Dependence of Electroluminescent Zinc Sulphide." *Philips Research Reports*. 10, 205-215, 1955.
17. Bhatti, H.S., N.K. Verma, and Sunil Kumar. "Life-Time Measurements of Doped Zinc Sulphide under Nitrogen Laser Excitation." *Indian Journal of Engineering and Materials Sciences*. 7, 461-463, 2000.
18. Gavryushin, V., R. Baltramiejunas, G. Raciukaitis, and A. Kazlauskas. "Nonlinear Spectroscopy of Deep Levels in ZnS Crystals." *Lithuanian Journal of Physics*. 37(6), 1-8, 1997.
19. Johnston, S.W., R.K. Ahrenkiel, D.J. Friedman, and S.R. Kurtz. "Temperature-Dependent Carrier Lifetime in GaNAs Using Resonant-Coupled Photoconductive Decay." NCPV Program Review Meeting. 263-264, 2001.
20. Osram Sylvania. "Type 728 Phosphor Luminescent Material." Technical Information Bulletin.

Approved for general distribution by Wayne Brown, 5/27/04

APPENDIX A: Wavelength Calculations for Hexagonal and Cubic Structures

Hexagonal Structure ZnS

$3.72\ eV\ [(1.602 * 10^{-19}) / 1\ ev] = [(6.63 * 10^{-34}\ J \cdot s) * (3.00 * 10^{8}\ m \cdot s^{-1})] / \lambda$

$5.95944 * 10^{-19}\ J = (1.989 * 10^{-25}\ J \cdot m) / \lambda$

$\lambda = 3.337 * 10^{-7}\ m * (1\ nm / 1 * 10^{-9}\ m)$

$\lambda = 333\ nm$

Cubic Structure ZnS

$3.64\ eV\ [(1.602 * 10^{-19}) / 1\ ev] = [(6.63 * 10^{-34}\ J \cdot s) * (3.00 * 10^{8}\ m \cdot s^{-1})] / \lambda$

$5.83128 * 10^{-19}\ J = (1.989 * 10^{-25}\ J \cdot m) / \lambda$

$\lambda = 3.411 * 10^{-7}\ m * (1\ nm / 1 * 10^{-9}\ m)$

$\lambda = 341\ nm$

APPENDIX B: RAW SPECTROSCOPIC DATA

Emission Spectra Data for 200 Hz

Wavelength (nm)	Intensity (Volts)
300	0.03765
310	0.04085
320	0.01185
330	0.01393
340	0.00685
350	0.01486
360	0.02306
370	0.00000
380	0.008568
390	-0.0007
400	0.011189
410	0.016879
420	0.035756
430	0.074070
440	0.145888
450	0.272398
460	0.496348
470	0.734568
480	1.003008
490	1.050418
500	1.095248
510	1.032038
520	0.890798
530	0.719248
540	0.537038
550	0.354428
560	0.233908
570	0.144768
580	0.074853
590	0.044660
600	0.019053
610	0.003005
620	-0.010278
630	-0.018477
640	-0.016479
650	-0.023896
660	-0.016799
670	-0.022266
680	-0.019740
690	-0.025526
700	-0.020891

APPENDIX C: RAW SPECTROSCOPIC DATA

Emission Spectra Data for 1500 Hz

Wavelength (nm)	Intensity (Volts)
300	-0.12414
310	-0.124252
320	-0.118466
330	-0.114118
340	-0.118002
350	-0.117011
360	-0.122685
370	-0.123548
380	-0.123437
390	-0.118162
400	-0.09182
410	0.06738
420	0.056787
430	1.42865
440	2.45565
450	3.44007
460	4.42064
470	5.27628
480	5.87668
490	6.27638
500	6.06843
510	5.43352
520	4.62647
530	3.55143
540	2.53337
550	1.7052
560	1.08559
570	0.64479
580	0.3394
590	0.14569
600	0.03522
610	-0.022146
620	-0.059676
630	-0.0870341
640	-0.098837
650	-0.101714
660	-0.111624
670	-0.11367
680	-0.109499
690	-0.115013
700	-0.11204

APPENDIX D: RAW SPECTROSCOPIC DATA

Emission Spectra Data for 20 kHz

Wavelength (nm)	Intensity (Volts)
300	-0.117522
310	-0.11781
320	-0.113399
330	-0.123804
340	-0.118066
350	-0.116004
360	-0.118018
370	-0.116947
380	-0.120975
390	-0.111193
400	-0.0435
410	0.43717
420	1.88456
430	4.42379
440	6.78143
450	8.17379
460	8.2157
470	7.63946
480	6.56876
490	5.57121
500	4.61856
510	3.79331
520	2.72349
530	2.01952
540	1.43009
550	0.94072
560	0.60034
570	0.32261
580	0.15652
590	0.04342
600	-0.011932
610	-0.055249
620	-0.081894
630	-0.097063
640	-0.097287
650	-0.105231
660	-0.104991
670	-0.107996
680	-0.114134
690	-0.116755
700	-0.11383

APPENDIX E: Calculations of Experimental Lifetime of 200 Hz and 1500 Hz

200 Hz 480 nm

$$t_{1/2} = \frac{0.693}{3425.8}$$

$$= 0.0002023 \text{ seconds}$$

200 Hz 515 nm

$$t_{1/2} = \frac{0.693}{3204.1}$$

$$= 0.0002163 \text{ seconds}$$

1500 Hz 470 nm

$$t_{1/2} = \frac{0.693}{5309.7}$$

$$= 0.0001305 \text{ seconds}$$

1500 Hz 510 nm

$$t_{1/2} = \frac{0.693}{3813.6}$$

$$= 0.0001817 \text{ seconds}$$